

Full-Duplex Spectrum Sensing in Broadband Power Line Communications

Gautham Prasad and Lutz Lampe

Department of Electrical and Computer Engineering

The University of British Columbia, Vancouver, BC

Email: gauthamp@ece.ubc.ca

Abstract—We address the issue of electromagnetic interference between power line communication (PLC) and non-PLC services by using full-duplex spectrum sensing for cognitive PLC. Contemporary broadband PLC (BB-PLC) standards allow PLC devices to dynamically use idle spectra that are allotted to non-PLC services, like broadcast radio. Traditional spectrum sensing techniques operate in a half-duplex manner, and thus provide sub-optimal sensing efficiency. In this paper, we propose the use of in-band full-duplex (IBFD) operation to allow simultaneous data transmission and spectrum sensing, and eliminate all sensing-only and other wait times involved in conventional spectrum sensing operations. We first show that using the state-of-the-art IBFD solution yields inaccurate spectrum sensing performance due to non-negligible residual self-interference. We therefore propose multiple solutions to address this problem. We show through simulation results that our proposed solutions provide sufficient self-interference cancellation to achieve nearly the same spectrum sensing accuracy as that obtained in a half-duplex operation.

Index Terms—Cognitive PLC, dynamic spectrum management, smart notching, dynamic notching, in-band full duplex (IBFD)

I. INTRODUCTION AND MOTIVATION

Unshielded power lines are susceptible to electromagnetic interference (EMI) from the surrounding environment [1, Ch. 3]. Consequently, power line communication (PLC) signals also cause undesired EMI with non-PLC services in overlapping frequency bands. Many non-PLC services, like broadcast, amateur, and citizens band radio, operate in the frequency band of 2-100 MHz that is used for broadband PLC (BB-PLC). To protect these services, regulatory authorities restrict BB-PLC devices from using most of these frequencies. BB-PLC standards comply with these regulations and enforce a transmission tone-mask consisting of several intermediate spectral notches [2, Ch. 4]. Since these bands are frequently idle, permanent notching wastes valuable spectral resources.

Newer BB-PLC standards, like EN 50561-1, allow the use of dynamic notching to utilize the spectra allotted to broadcast radio services whenever they are idle [3]. Many cognitive PLC campaigns have been conducted to determine efficient strategies and criteria to detect the presence of these broadcast radio interferences [4]–[7]. However, all of them consider a half-duplex (HD) operation, where the PLC device suspends its transmission at regular intervals to sense the spectrum. We

define the efficiency, η , in such cases as $\eta = \frac{t_s}{T_p}$, where t_s is the time duration used by the secondary user (i.e., PLC transceiver) for data transmission, and T_p is the total time during which the primary user (i.e., broadcast radio transmitter) is inactive. Therefore, $T_p - t_s$ is the time spent on spectrum sensing, and other wait times. The efficiency of such systems can be increased if the secondary users develop the ability to sense the spectrum as well as transmit data at the same time on the line.

Full-duplex operation, which is more specifically referred to as in-band full-duplex (IBFD) operation, provides a means for BB-PLC transceivers to simultaneously transmit and receive data in the same frequency band over the same power line. Hence, IBFD provides a powerful technique to accomplish 100% efficiency in cognitive PLC scenarios by allowing spectrum sensing and data transmission at the same time. When combined with a signal-to-noise ratio (SNR) based interference detection method [7], IBFD enables PLC devices to transmit and receive data, as well as detect non-PLC interferences, all at the same time.

In our earlier works [8], [9], we have shown that IBFD can be accomplished for BB-PLC with the use of an operational amplifier based analog hybrid and a digital echo cancellation circuit to estimate and cancel the self-interference (SI). In this paper, we first use such a solution to achieve simultaneous data transmission and spectrum sensing. We adopt the standardized detection procedure detailed in EN 50561-1 and ETSI TS 102 578 [3], [10] to detect broadcast radio interferences. Using the IBFD implementation of [9], we show that under low noise floor conditions at the receiver, the performance of spectrum sensing with IBFD operation deteriorates from that under a half-duplex operation due to the effects of residual self-interference (RSI). We identify that this restriction is caused by the limited precision of the analog-to-digital converter (ADC) used at the receiver. To alleviate this constraint, we propose solutions that improve the dynamic range of the ADC, and reduce the power levels of the ADC input signal. We show the improvements in spectrum sensing performance achieved by our proposed solutions, through simulations performed under a limiting low noise floor condition. Further, we also compute throughput gains obtained under realistic BB-PLC channel and noise settings by using full-duplex dynamic notching in the broadcast radio bands.

The rest of the paper is organized as follows. In Section II, we describe the mechanism of spectrum sensing under IBFD operation. To counter the increase in the effective noise floor produced by the existing IBFD implementation, we propose multiple solutions in Section III. We present simulation results in Section IV to show the effectiveness of each of our solutions implemented independently. In Section V, we quantify the benefits obtained by using full-duplex dynamic notching in cognitive PLC. Finally, conclusions are drawn in Section VI.

II. SPECTRUM SENSING WITH IN-BAND FULL DUPLEXING

We perform spectrum sensing for broadcast radio services in the frequency domain by monitoring the PSD of the received signal. We use the detection criteria specified in ETSI TS 102 578 for HD operations [10], and adapt it to spectrum sensing with IBFD operation. The specification stipulates M specific broadcast radio bands to be monitored for the presence of a radio signal. Hence, we perform spectrum sensing in every m th radio band, for all $m = 1, 2, \dots, M$. A radio broadcast signal is considered to be present at a frequency f_k , if both the following conditions are met [10]:

$$\frac{N_R(f_k)}{\frac{1}{2|\mathcal{N}_m|} \left(N_R^{(\text{low},m)} + N_R^{(\text{high},m)} \right)} \geq \alpha_1 \quad (1)$$

$$N_R(f_k) \geq \alpha_2, \quad (2)$$

where

$$N_R^{(\text{low},m)} = \sum_{i=1}^{|\mathcal{N}_m|} N_R(f_{k_1^m} - i\Delta f), \quad (3)$$

$$N_R^{(\text{high},m)} = \sum_{i=1}^{|\mathcal{N}_m|} N_R(f_{k_{|\mathcal{N}_m|}^m} + i\Delta f), \quad (4)$$

N_R represents the PSD of the signal being monitored (i.e., in HD mode, it represents the noise floor PSD at the receiver), Δf is the spacing between two frequency bins, $\mathcal{N}_m = \{k_1^m, k_2^m, \dots, k_{|\mathcal{N}_m|}^m\}$ is the set of sub-carrier indices that lie in the m th pre-defined radio band with $k_i^m < k_{i+1}^m$, and $k \in \mathcal{N}_m$. $N_R^{(\text{low})}$ and $N_R^{(\text{high})}$ indicate the aggregate noise floor on either sides of the radio band (i.e., lower- and higher-ends), with values summed over a bandwidth equal to that of the radio band itself¹. The values in [10] specify $\alpha_1 = 10^{1.4}$ and $\alpha_2 = 10^{-13.5}$. Thus, (1) ensures that the detected interference is at least 14 dB above the noise floor on either side of the radio band, and (2) ensures that its power is at least -95 dBm in a bandwidth of 9 kHz, which translates to a PSD of $-95 \text{ dBm} - 10 \log_{10}(9 \text{ kHz}) \approx -135 \text{ dBm/Hz}$.

With the IBFD operation, the received signal contains not only the noise at the receiver, but also the RSI signal that is present due to non-ideal SI cancellation. Therefore, the average

¹In view of minimizing implementation complexity, we replace computing the median noise floor, as suggested in [10], with computing the mean instead in (3), (4), and (1), by enforcing no out-of-band radio interferences outside \mathcal{N}_m , $\forall m = 1, 2, \dots, M$, as suggested in [5].

noise floor on either side of the m th radio band is increased by a factor of

$$\gamma_m = 1 + \frac{P_{\text{RSI}}^{(\text{low},m)} + P_{\text{RSI}}^{(\text{high},m)}}{N_R^{(\text{low},m)} + N_R^{(\text{high},m)}}, \quad (5)$$

where

$$P_{\text{RSI}}^{(\text{low},m)} = \sum_{i=1}^{|\mathcal{N}_m|} P_{\text{RSI}}(f_{k_1^m} - i\Delta f),$$

$$P_{\text{RSI}}^{(\text{high},m)} = \sum_{i=1}^{|\mathcal{N}_m|} P_{\text{RSI}}(f_{k_{|\mathcal{N}_m|}^m} + i\Delta f),$$

and P_{RSI} represents the RSI PSD including any effects introduced due to the RSI, such as additional distortion and quantization noise. This increase in noise floor affects condition (1), which examines the relative power level of a potential radio interference to the adjacent noise floor. By applying the HD threshold of α_1 for IBFD operations, we increase the probability of missed detections, as we fail to detect interferences with PSD levels from $\frac{\alpha_1}{2|\mathcal{N}_m|} \left(N_R^{(\text{low},m)} + N_R^{(\text{high},m)} \right)$ to $\frac{\alpha_1 \gamma_m}{2|\mathcal{N}_m|} \left(N_R^{(\text{low},m)} + N_R^{(\text{high},m)} \right)$. Alternatively, to maintain the same probability of missed detections as that obtained in HD operations, we are required to determine a new $\alpha_1' \leq \alpha_1$ for every m th radio band, based on the value of γ_m . This results in a possible increase in false alarm rates, as non-broadcast radio interferences could be detected as one, due to a reduced verification threshold. An increase in false alarm rates partially defeats the purpose of dynamic notching. Additionally, γ_m dynamically varies with changes in PLC channel conditions as the extent of SI cancellation provided by the IBFD solution varies with change in the network impedance [9]. Furthermore, determining the value of γ_m would require an accurate estimation of $N_R^{(\text{low},m)}$ and $N_R^{(\text{high},m)}$ at every m th radio band regularly, which in turn requires a silent period (i.e., HD operation). Therefore, to address these issues, we propose solutions in the next section that accomplish $\gamma_m \approx 1$ for all $m = 1, 2, \dots, M$.

III. PROPOSED SOLUTIONS

The IBFD solution presented in [9] uses an op-amp based hybrid for passive isolation and a digital cancellation procedure for active SI cancellation. Since the hybrid isolation is relatively weak, the SI is not sufficiently attenuated to produce benign values of distortion and quantization noise at the ADC. Hence, under low noise conditions at the receiver, it can be seen from (5) that this potentially produces $\gamma_m \gg 1$. The distortion and quantization noise power introduced by the ADC is given by

$$P_{\text{ADC}} = \frac{P_{\text{inp}}}{\text{SDQNR}}, \quad (6)$$

where P_{inp} is the power of the input signal entering the ADC, and SDQNR is the signal-to-distortion-plus-quantization-noise ratio of the ADC. Thus, to reduce P_{ADC} , we propose three different solutions in the following, each of which either reduces P_{inp} or increases SDQNR.

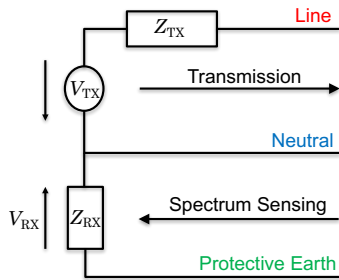


Fig. 1. Structure of one configuration of our proposed two conductor-pair spectrum sensing solution.

A. Improving ADC SDQNR

Our first solution is fairly straightforward and attempts to increase SDQNR provided by an ADC. The ADC in the receiver chain is preceded by an automatic gain control (AGC) block that scales the input signal such that it occupies the entire dynamic range of the ADC. However, since OFDM signals possess a high peak-to-average-power ratio, the AGC scales the input signal to accommodate some clipping, in order to minimize the overall clipping distortion and quantization noise [11]. Under such an operation, the SDQNR of the ADC is given by [12]

$$\text{SDQNR}^{-1} = \frac{1}{2^{2b}} \left(\frac{V_{\text{clip}}}{\sigma_{\text{inp}}} \right)^2 + \sqrt{\frac{8}{\pi}} \left(\frac{\sigma_{\text{inp}}}{V_{\text{clip}}} \right)^3 \exp\left(\frac{-V_{\text{clip}}^2}{2\sigma_{\text{inp}}^2}\right), \quad (7)$$

where b is the number of ADC bits, σ_{inp}^2 is the variance of the input signal, and V_{clip} is the voltage beyond which the signal is clipped. It has been shown in [13] that there exists an optimal $\left(\frac{V_{\text{clip}}}{\sigma_{\text{inp}}}\right)$ for every b , which maximizes SDQNR. Therefore, by tuning the AGC to provide the ADC with the optimal $\left(\frac{V_{\text{clip}}}{\sigma_{\text{inp}}}\right)$, the only other avenue to improve SDQNR further is by increasing b . We show later in Section IV that by using a 16-bit ADC in place of the default 12-bit resolution that current BB-PLC devices use, we nearly achieve $\gamma_m \approx 1$.

We recognize that increasing ADC precision to improve SDQNR is a fairly simplistic solution that introduces additional complexity to the transceiver chip-set. Therefore, we proceed to present two other solutions that attempt to reduce P_{inp} , to thereby decrease P_{ADC} .

B. Increasing Passive Isolation

As our second solution, we propose a method to decrease P_{inp} by improving the passive isolation provided at the line-device interface. The IBFD solution proposed in [9] achieves passive isolation using a three-port hybrid circuit. One of the ports is connected to the power line channel and the other two to the transmitter and receiver chains of the transceiver front-end. The isolation obtained using this circuit is given by

$$I_{\text{hyb}}(f) = \frac{c}{|\Gamma(f)|^2}, \quad (8)$$

where c is a scaling factor capturing the extent of impedance bridging and matching at the hybrid ports connected to the

transmitter and receiver ends of the transceiver, respectively, and $\Gamma(f) = \frac{Z_{\text{PLC}}(f) - Z_{\text{hyb}}}{Z_{\text{PLC}}(f) + Z_{\text{hyb}}}$ is the reflection co-efficient at the line-hybrid interface at a frequency f , with a line impedance of Z_{PLC} and a hybrid port impedance of Z_{hyb} . Since the constant resistive Z_{hyb} is often mismatched to a widely varying complex Z_{PLC} , $I_{\text{hyb}}(f)$ obtained is relatively weak [9]. This results in P_{inp} that is large enough to produce $\gamma_m \gg 1$ under low N_R conditions. Thus, we propose the following solution to increase the passive isolation.

Many in-home wiring installations consist of three wires, line, neutral, and protective earth, for power distribution [14, Ch. 1.2]. By using one of the pairs for transmission, and another for spectrum sensing, we achieve higher passive isolation of SI at the line-device interface without the use of a hybrid. A conceptual structure of this setup is shown in Fig. 1. The passive isolation obtained under this scenario is expressed as

$$I_{\text{pas}}(f) = \left| \frac{V_{\text{RX}}(f)}{V_{\text{TX}}(f)} \right|^{-2}, \quad (9)$$

where V_{TX} and V_{RX} are the voltages at the transmitter and receiver ends of the device, respectively. By viewing this setup as a two-port network, with the Z-parameters of the network represented by the effective input power line impedance matrix, \mathbf{Z}_{PLC} , we obtain

$$\frac{V_{\text{RX}}}{V_{\text{TX}}} = \frac{Z_{\text{PLC},ji} Z_{\text{RX}}}{(Z_{\text{TX}} + Z_{\text{PLC},ii})(Z_{\text{RX}} + Z_{\text{PLC},jj}) - Z_{\text{PLC},ij} Z_{\text{PLC},ji}}, \quad (10)$$

where $Z_{\text{PLC},ij}$ is the (i, j) th element of \mathbf{Z}_{PLC} with the transmitter and receiver connected to the i th and j th conductor pairs, respectively, and Z_{TX} and Z_{RX} are the device front-end impedances of the transmitter and receiver chains, respectively. We drop the index f for brevity. We show through numerical results in Section IV that this setup improves the passive isolation over that obtained in [9], without using a hybrid. However, we find that this isolation is insufficient to provide $\gamma_m \approx 1$. We also recognize that this solution uses an additional resource (wire-pair) to accomplish a single-input single-output (SISO) communication. Thus, we attempt to reduce P_{inp} using active cancellation in the following.

C. Analog Active Cancellation

The third solution we propose to reduce P_{ADC} is based on the introduction of active analog SI cancellation. Active cancellation involves generating an SI estimate, and canceling it from the interference-affected received signal. Active cancellation in the existing IBFD solution is completely realized digitally [9]. Alternatively, by canceling SI from the received signal in the analog domain, P_{inp} can significantly be reduced due to higher pre-digital cancellations.

We use the IBFD solution in [9] as a foundation to propose our analog cancellation (AC) structure. The solution in [9] uses the digital samples of the received signal to train a set of filter weights using the least mean squares algorithm, in the frequency domain. It then generates digital echo estimate samples in time domain to cancel from the received signal.

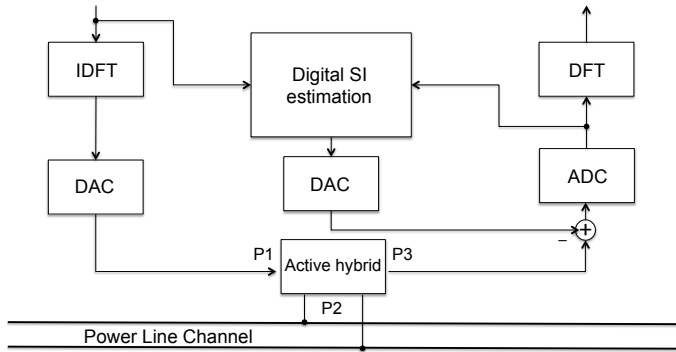


Fig. 2. A conceptual block diagram of our proposed active analog cancellation solution.

TABLE I
SIMULATION PARAMETERS

Transmission bandwidth	2 – 28 MHz
Sampling frequency	75 MHz
FFT Size	3072
Number of data carrying sub-carriers	917
Sub-carrier spacing	24.414 kHz
Transmit PSD	-50 dBm/Hz
Spectrum Sensing RBW (Δf)	300 Hz
Number of AM interferences	10
Number of DRM interferences	10

We use a similar setup, but with an additional digital-to-analog converter in the echo reconstruction chain to generate an analog SI estimate. We then cancel the SI estimate from the received signal in analog domain before it reaches the ADC. A schematic overview of this solution is shown in Fig. 2. Due to lack of space, we provide implementation details, motivations for the choice of such an AC scheme, and detailed performance analysis of our solution in [15]. However, we show its impact on full-duplex spectrum sensing in the following section.

IV. NUMERICAL RESULTS

A. Simulation Configuration

1) *Transceiver Settings*: We consider a BB-PLC transceiver that operates as per HomePlug AV specifications [2]. We transmit in a bandwidth of 2 – 28 MHz, and apply the permanent tone-mask specified in [16] to notch out intermediate frequencies that overlap with the HAM bands of amateur radio. We use a 3072-point fast Fourier transform (FFT) to load data on to 917 orthogonal sub-carriers with a sampling rate of 75 MHz. Furthermore, we adopt the North American amplitude mask to transmit with a maximum PSD of -50 dBm/Hz on all data carrying sub-carriers [2]. For spectrum sensing, we choose an FFT size that provides a resolution bandwidth (RBW) of 300 Hz as recommended by [10]. We summarize the simulation parameters in Table I. For all our simulations using a b -bit ADC, we operate with an optimal clipping ratio of $\left(\frac{V_{clip}}{\sigma_{imp}}\right)_{opt} = -0.0053b^2 + 0.3763b + 1.2627$ [13].

2) *Channel and Noise Generation*: We use the channel generator tools of [17] and [18] to realize random realistic indoor channels. Since the performance of IBFD spectrum

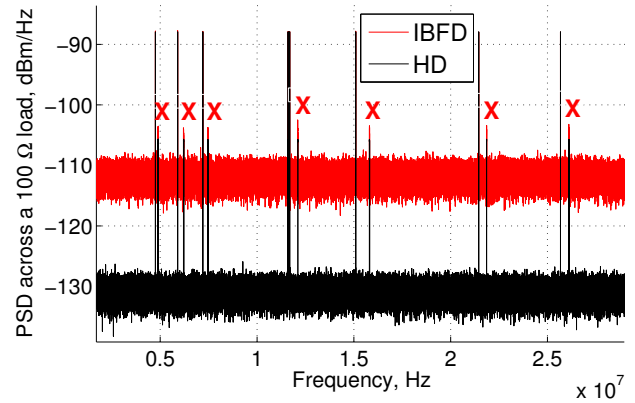


Fig. 3. PSD of the monitored signal under HD and IBFD operations using the IBFD implementation of [9]. A cross (X) on top of a peak indicates that the IBFD implementation fails to satisfy condition (1).

sensing deteriorates as γ_m increases, we use a white noise of $N_R = -130$ dBm/Hz to simulate a low-noise environment.

3) *Broadcast Radio Interferences*: We use an interference signal with 10 amplitude modulation (AM) radio and 10 digital radio mondiale (DRM) interferences. We adopt the test signal provided in [10], which contains interferences near the borders of the pre-defined radio bands to test the effectiveness of our spectrum sensing procedure. However, we reduce the interference amplitudes to demonstrate the impact of the increased noise floor under IBFD operation. Each of the AM and DRM interferences in the signal appear in pairs in the frequency domain, i.e., the signal contains 10 pairs of interferences, with every pair containing an AM signal of a larger amplitude and a DRM signal of a smaller amplitude.

B. Simulation Results

1) *Increased Noise Floor*: Our first result in Fig. 3 shows the impact of IBFD operation on spectrum sensing using the state-of-the-art IBFD solution from [9]. As this solution is limited by the ADC dynamic range, it provides a maximum SI cancellation gain of about 63 dB. Therefore, the PSD floor of the monitored signal in IBFD mode is around -113 dBm/Hz, which produces $\gamma_m \approx 50$. With the specified $\alpha_1 = 10^{1.4}$ [10], any interference between -116 dBm/Hz and -99 dBm/Hz satisfies condition (1) only with HD spectrum sensing but not with IBFD. As a result, we observe in Fig. 3 that spectrum sensing fails to detect interferences corresponding to DRM signals.

2) *Impact of Higher Precision ADCs*: Fig. 4 shows the results of our first solution. We use ADCs of varying precision at the receiver along with the IBFD solution of [9]. Increasing the ADC precision provides higher SDQNR of the ADC. Therefore, the resultant distortion and quantization noise is reduced. This ensures that P_{ADC} limiting the cancellation gain obtained by [9] is maintained at a lower level to provide higher digital cancellation gains. We observe from Fig. 4 that by using the default 12-bit ADC, we obtain an increased noise floor, as also evident in Fig. 3. However, with a 16-bit ADC, we achieve

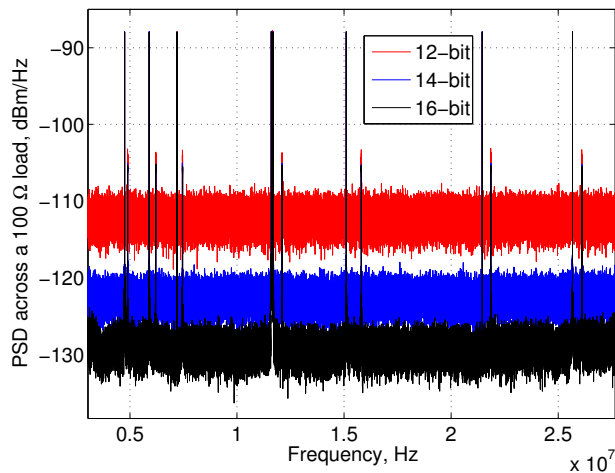


Fig. 4. PSD of the monitored signal under IBFD operation with 12-, 14-, and 16-bit ADCs.

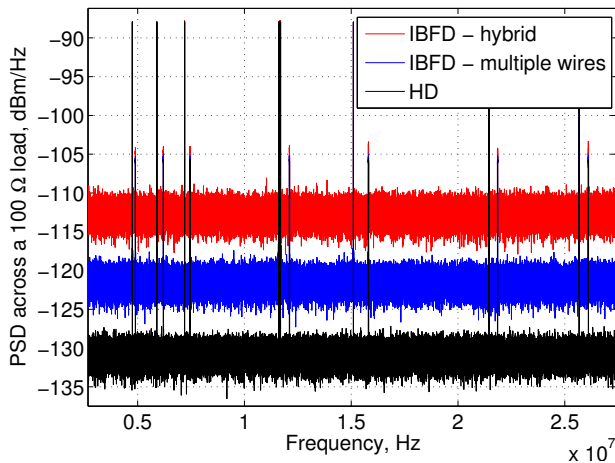


Fig. 5. PSD of the monitored signal under HD operation, IBFD using the two conductor-pair setup for passive isolation, and IBFD with the hybrid [9].

$P_{RSI} \approx -130$ dBm/Hz, producing $\gamma_m < 2$. Although this value is sufficient to produce accurate spectrum sensing under all scenarios with a suitable α_1 , deployment of this solution requires new chip-sets of increased complexity with higher precision ADCs.

3) *Increase in Passive Isolation with an Additional Conductor Pair*: The result of our second proposed solution can be seen in Fig. 5. We design a coupling interface where we use one conductor pair for data transmission and another for spectrum sensing considering a three-conductor channel generated using [18]. We persist with the digital cancellation procedure of [9] for active cancellation. The SI signal undergoes passive isolation at the line-device interface due to coupling losses between the two conductor-pairs. Our simulation results indicate a typical passive isolation of the two conductor-pair setup to be around 14 dB, which is more than five times the passive isolation gain provided by the hybrid used in [9]. However, we observe from Fig. 5 that we do not achieve $\gamma_m \approx 1$ as the

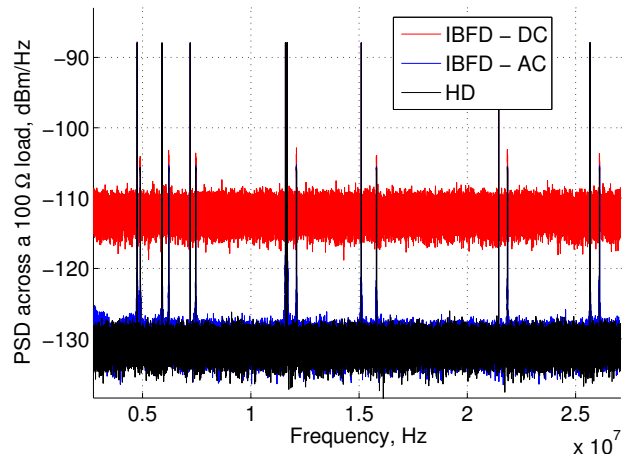


Fig. 6. PSD of the monitored signal under HD operation, IBFD with the active digital cancellation (DC) solution of [9], and the proposed IBFD solution with AC.

PSD of the monitoring signal is still about 10 dB above the noise floor.

4) *Increase in Active Cancellation Gain with Analog Cancellation*: We finally present the result of our third proposed solution in Fig. 6, where we compare the accuracy of spectrum sensing using our proposed AC method with the IBFD solution of [9] and the HD operation. Since we operate with analog signals in our proposed method, we use the default 64-bit double precision of MATLAB to simulate an infinite precision analog signal, and use a 12-bit ADC for digitizing. The results in Fig. 6 show that the PSD of the monitored signal in IBFD operation using our proposed AC solution is nearly the same as that under HD operation. This signifies $\gamma_m \approx 1$, which indicates the same spectrum sensing accuracy in both HD and IBFD-with-AC operations. We also note that our AC solution can be implemented without the hybrid by using a two conductor-pair setup to achieve passive isolation.

V. QUANTIFYING THE GAINS

A. Increase in Throughput

The increase in throughput by using dynamic notching is directly proportional to the bandwidth allotted to broadcast radio services. EN 50561-1 specifies a pre-defined set \mathcal{N}_m , covering a total bandwidth of 5.8 MHz, in which transmission sub-carriers can either be permanently or dynamically notched out by PLC transceivers depending on the spectrum sensing ability of the device. We compute the maximum throughput gained by using all sub-carriers in \mathcal{N}_m as

$$C = \sum_{m \in \mathcal{N}_m} \int_{f_{k_1^m}}^{f_{k_{|\mathcal{N}_m|}^m}} \log_2 \left(1 + \frac{P_{TX}(f) |H_{PLC}(f)|^2}{P_{RSI}(f) + N_R(f)} \right) df, \quad (11)$$

where P_{TX} is the transmit PSD used by the PLC device and H_{PLC} is the power line channel transfer function. To obtain realistic values of C , we limit the maximum modulation order

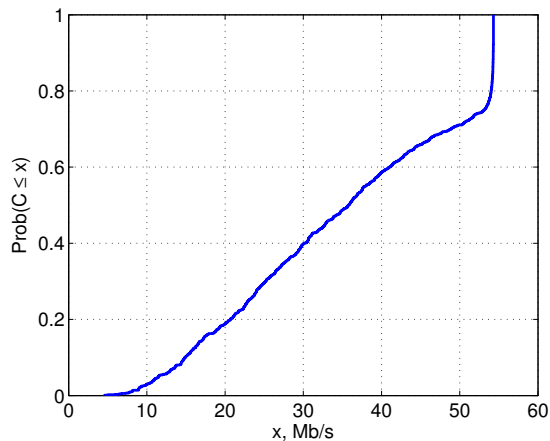


Fig. 7. CDF of throughput gained by using broadcast radio bands.

to 1024-QAM as per HomePlug AV specifications [2], and also allow a guard band of 12 kHz at either ends of a broadcast band to emulate practical notching abilities of band-pass filters.

We compute (11) for 1500 random PLC channel and noise conditions that we generate using the random network setting in [17] and [19]. By achieving $\gamma_m \approx 1$, we let $P_{RSI}(f) + N_R(f) \approx N_R(f)$ for all $2 \text{ MHz} \leq f \leq 28 \text{ MHz}$ in our computations. The empirical cumulative distribution function (CDF) plot of the resultant throughput gains are shown in Fig. 7. We observe that we obtain a maximum throughput gain of up to 53 Mb/s, with a median of about 35 Mb/s.

B. Increase in Spectrum Sensing Efficiency

The maximum throughput gain computed in Section V-A is only applicable when all the broadcast radio bands are idle for use by PLC devices. During this interval, only a portion of this time, η , as defined in Section I, is used for actual data transmission. Using our proposed IBFD spectrum sensing techniques, we achieve the optimal efficiency of $\eta_{FD} = 1$, as we transmit and sense the medium simultaneously at all times. In contrast, a portion of this total time is consumed by sensing-only operations in a HD operation. Spectrum sensing timings have not been comprehensively tested and are not strictly enforced. Practical sensing-only and other wait times in HD spectrum sensing are dependent on the typical coherence time of the surrounding wireless environment in the broadcast radio bands. Using the values suggested for possible sensing times in [10, Sec. 4.2], the efficiency could be as low as, $\eta_{HD} = 0.3$. Under such conditions, we obtain over a three-time increase in ergodic throughput gain using IBFD spectrum sensing over the HD operation.

VI. CONCLUSIONS

In this paper, we have proposed solutions to counter the impact of residual self-interference on full-duplex spectrum sensing. We showed through analysis and simulation results that we observe an increase in PSD of the monitored signal

when using the state-of-art IBFD implementation. Recognizing that this limitation is imposed due to inadequate dynamic range of the ADC, we proposed solutions to counter this constraint by either increasing SDQNR of the ADC, or by reducing the power of the input signal entering the ADC. We demonstrated through simulation results that our proposed solutions overcome the restriction of limited ADC precision to provide nearly identical spectrum sensing accuracy as that achieved with HD operation. Due to the ability to transmit and sense the medium simultaneously using IBFD operation, we achieved the maximum spectrum sensing efficiency of 100%.

REFERENCES

- [1] L. Lampe, A. M. Tonello, and T. G. Swart, *Power Line Communications: Principles, Standards and Applications from Multimedia to Smart Grid*, 2nd ed. John Wiley & Sons, 2016.
- [2] H. A. Latchman, S. Katar, L. Yonge, and S. Gavette, *Homeplug AV and IEEE 1901: A Handbook for PLC Designers and Users*. Wiley-IEEE Press, 2013.
- [3] A. Schwager, "Cognitive frequency exclusion in EN 50561-1:2012," in *MIMO Power Line Communications: Narrow and Broadband Standards, EMC, and Advanced Processing*, L. T. Berger, A. Schwager, P. Pagani, and D. M. Schneider, Eds. CRC Press, 2014, ch. 22, pp. 601–624.
- [4] B. Praho, M. Tlich, P. Pagani, A. Zeddani, and F. Nouvel, "Cognitive detection method of radio frequencies on power line networks," in *IEEE Intl. Symp. Power Line Commun. Appl. (ISPLC)*, 2010, pp. 225–230.
- [5] Y. Lu, W. Liu, J. Li, and H. Gao, "Measurement and cognitive detection method of broadcast radio stations in distribution networks," in *IEEE Intl. Symp. Power Line Commun. Appl. (ISPLC)*, 2014, pp. 75–80.
- [6] A. Schwager, "Powerline communications: Significant technologies to become ready for integration," Ph.D. dissertation, Universitat Duisburg-Essen, 2010.
- [7] N. Weling, "SNR-based detection of broadcast radio stations on powerlines as mitigation method toward a cognitive PLC solution," in *IEEE Intl. Symp. Power Line Commun. Appl. (ISPLC)*, 2012, pp. 52–59.
- [8] G. Prasad, L. Lampe, and S. Shekhar, "Enhancing transmission efficiency of broadband PLC systems with in-band full duplexing," in *IEEE Intl. Symp. Power Line Commun. and Its Appl. (ISPLC)*, March 2016.
- [9] —, "In-band full duplex broadband power line communications," *IEEE Trans. Commun.*, vol. 64, no. 9, pp. 3915–3931, Sept 2016.
- [10] ETSI TS 102 578 v1.2.1, "PowerLine Telecommunications (PLT): Coexistence between PLT modems and Short Wave Radio Broadcasting Services," 2008.
- [11] D. Dardari, "Joint clip and quantization effects characterization in OFDM receivers," *IEEE Trans. Circuits Syst. I: Regular Papers*, vol. 53, no. 8, pp. 1741–1748, 2006.
- [12] D. J. Mestdagh, P. M. Spruyt, and B. Biran, "Effect of amplitude clipping in DMT-ADSL transceivers," *IET Electronics Letters*, vol. 29, no. 15, pp. 1354–1355, 1993.
- [13] H. Ehm, S. Winter, and R. Weigel, "Analytic quantization modeling of OFDM signals using normal Gaussian distribution," in *Asia-Pacific Microwave Conference*, Dec 2006, pp. 847–850.
- [14] L. T. Berger, A. Schwager, P. Pagani, and D. Schneider, *MIMO Power Line Communications: Narrow and Broadband Standards, EMC, and Advanced Processing*. CRC Press, 2014.
- [15] G. Prasad, L. Lampe, and S. Shekhar, "Analog interference cancellation for full-duplex broadband power line communications," in *IEEE Intl. Symp. on Power Line Commun. Appl. (ISPLC)*, Apr 2017.
- [16] "Homeplug AV specification, version 1.1," *HomePlug Powerline Alliance*, pp. 1 – 673, May 2007.
- [17] G. Marrocco, D. Statovci, and S. Trautmann, "A PLC broadband channel simulator for indoor communications," in *IEEE Intl. Symp. Power Line Commun. and Its Appl. (ISPLC)*, 2013, pp. 321–326.
- [18] F. Gruber and L. Lampe, "On PLC channel emulation via transmission line theory," in *IEEE Intl. Symp. Power Line Commun. and Its Appl. (ISPLC)*, Austin, TX, USA, 2015. [Online]. Available: <http://www.ece.ubc.ca/lampe/MIMOPLC>
- [19] G. Prasad, H. Ma, M. J. Rahman, F. Aalamifar, and L. Lampe, (2016) A cumulative power line noise generator. [Online]. Available: <http://www.ece.ubc.ca/~gauthamp/PLCnoise>